The Bacteriophage ø29 Portal Motor can Package DNA Against a Large Internal Force

Douglas E. Smith[*¶], Sander J. Tans[*¶], Steven B. Smith[†], Shelley Grimes[‡], Dwight L. Anderson[‡], and Carlos Bustamante[*†§‖]

[*]*Department of Physics, University of California, Berkeley, CA 94720, U.S.A.*

[†]*Howard Hughes Medical Institute*

[‡]*Departments of Microbiology and Dentistry, University of Minnesota, Minneapolis, MN 55455, U.S.A.*

[§]*Department of Molecular and Cell Biology, University of California, Berkeley, CA 94720, U.S.A.*

[‖]*Physical Biosciences Division, Lawrence Berkeley Laboratory, Berkeley, CA 94720*

[¶] *These authors contributed equally to this work.*

As part of their infection cycle, viruses must package their newly replicated genomes for delivery to other host cells. Bacteriophage ø29 packages its 6.6 μm long double-stranded DNA into a 42 nm x 54 nm capsid[1] via a portal complex that hydrolyses ATP[2]. This process is remarkable because entropic, electrostatic, and bending energies of the DNA must be overcome to package the DNA to near-crystalline density. Here we use optical tweezers to pull on single DNA molecules as they are packaged, thus demonstrating that the portal complex is a force generating motor. This motor can work against loads of up to ~57 picoNewtons on average, making it one of the strongest molecular motors ever reported. Movements of over 5 μm are observed, indicating high processivity. Pauses and slips also occur, particularly at higher forces. We establish the force-velocity relationship of the motor and find that the rate-limiting step of the motor's cycle is force dependent even at low loads. Interestingly, the packaging rate decreases as the prohead is filled, indicating that an internal force builds up to 50 pN due to DNA confinement. Our data suggest that this force may be available for initiating the ejection of the DNA from the capsid during infection.

The *Bacillus subtilis* phage ø29 is an excellent model system for studying viral assembly[3]. The 19.3 kilobase genome with its terminal proteins, gp3, is packaged into a preformed capsid (prohead) in an efficient *in vitro* assay[4,5]. The motor lies at a unique portal vertex of the prohead[1,6,7] and contains: 1) the head-tail connector, a dodecamer of gp10 whose structure has been recently solved by X-ray crystallography[6]; 2) the prohead shell; 3) a ring of 174-base prohead RNAs (pRNA) which surrounds the protruding narrow end of the connector; and 4) an oligomer of gp16, an ATPase that first binds DNA-gp3 and then assembles onto the connector/pRNA complex prior to packaging. It has been hypothesized that this portal complex represents a new class of rotary molecular motors that couple rotation to DNA translocation[6].

Previously, bacteriophage DNA packaging has been studied in bulk reactions using DNase protection assays[4,5]. Here we present a new assay in which force-measuring optical tweezers are used to follow packaging activity of a single complex in real time. Stalled, partly-prepackaged complexes are attached to a polystyrene microsphere via the unpackaged end of the DNA (see methods). This microsphere is captured in the optical trap and brought into contact with a second microsphere, which is covered with phage antibodies and held by a pipette, to form a stable tether (Fig. 1a). In the absence of ATP, the tether displays the elasticity expected for a single DNA molecule[8]. Shortly after addition of ATP, the two microspheres are seen to move closer together, indicating packaging activity. Control experiments confirm this observation: 1. Proheads bound to antibody-coated microspheres efficiently package biotinylated ø29 DNA in a bulk assay; 2. No movement is observed when the proheads are omitted and the DNA is directly attached in the optical tweezers measurements; and 3. Packaging could be reversibly stalled by a non-hydrolyzable ATP analog (γS-ATP).

The first set of measurements was done in "constant force feedback" mode, in which the microsphere distance is adjusted by feedback to maintain DNA tension at a preset value of ~5 pN (Fig. 1a). Fig. 1b shows plots of the tether length versus time, for a ø29-λ DNA construct with a length of 1.8x the ø29 genome (see methods). In all measurements a saturating concentration of ATP was used (0.5 mM). Packaging is highly efficient: In over 95% of the measurements movements of several μm could be followed. Packaging dynamics are recorded with more detail, accuracy, and time resolution than has

been possible in bulk studies. Accounting for the prepackaging, we find that it takes 5.5 min. on average to package an amount equal to the ø29 genome, with a standard deviation from complex to complex of 0.8 min. A single complex also exhibits packaging rate fluctuations of ~20 bp/s RMS in a ~1 Hz bandwidth (Fig. 1c) that are ~5x larger than the measurement noise of ~4 bp/s RMS, determined when the DNA alone is directly attached between two beads (see supplemental data, Fig. I). Pauses in movement of variable duration (see Fig. 1b, inset) and slips (see below) are also clearly evident.

On average there are 3.1 pauses per μm of DNA packaged (σ=3.5, 43 complexes). At higher capsid fillings the pausing frequency increases (correlation coefficient[9] ≈ 0.8; also see supplemental data, Fig. III), although the pause duration is not strongly correlated with filling (correlation coefficient ≈ 0.01). During a pause, the DNA tether length remains constant despite the applied force, indicating that the motor stays engaged with the DNA. During packaging however, some complexes occasionally exhibit abrupt increases in DNA tether length (see Fig. 2, inset). Apparently the motor loses grip on the DNA but can grasp the molecule again and resume packaging immediately. The mean length of a slip is 44 bp, with a large standard deviation of σ=103 bp (n=99). We have not found any evidence that slips occur at specific locations along the DNA, but they do occur more often at higher applied forces (see supplemental data, Fig. IV). The motor is highly processive, in the sense that for the ensemble of records the length of DNA packaged divided by the number of slips is large (~7 μm, under a load of 5 pN).

In Fig. 1c the packaging rate is plotted vs. the percentage of the genome that has been packaged. Surprisingly these measurements show a dramatic reduction in packaging rate beginning when ~50% of the genome is packaged. Initially the rate is ~100 bp/s and it gradually drops down to zero as the capsid fills up and the motor stalls. Note that the proheads are able to package up to ~5% more DNA than the normal ø29 genome length. These observations suggest that the rate decrease results from the build up of an internal pressure due to DNA confinement, which exerts an opposing force and slows the motor.

To determine the internal force generated inside the capsid from the velocity changes observed, we must first establish how force affects the velocity of the motor. The force dependence of the motor was characterized using a “no feedback” mode where the positions of the trap and pipette are fixed (see Fig. 1a). These measurements were done

using ø29-*Nco*I-A DNA (0.8x the ø29 genome, see methods). In this mode the tension in the molecule increases as the motor reels in the DNA (Fig. 2a), and the bead is displaced from the trap center. This force acts directly on the motor, and at a certain point causes it to stall. These data thus reveal how the packaging rate depends on applied force. Fig. 3a shows three such Force-Velocity (*F-V*) traces for different complexes. The curve shapes are similar, although the initial packaging rate and the stall force vary somewhat.

The mean *F-V* behavior is obtained by first normalizing a number of individual curves to the mean stall force and mean initial velocity, and then averaging them together. Mean F-V curves were obtained at two points: when 1/3 and when 2/3 of the genome is packaged (Fig. 3b, red line and leftmost blue line, respectively). Fig 1c suggests that in the 1/3 case no significant internal force opposes the motor because the velocity has not yet been reduced by DNA filling, although the motor *does* exhibit sensitivity to external force even at these low fillings (Fig. 3b). *F-V* data in the 2/3 case, however, suggest that an internal force of ~14 pN must be acting on the motor, since it takes 14 pN less external force to stall the motor in this case (Fig. 3b). This inference relies on the supposition that the internal and external forces add together to act on the motor. This supposition is supported by the good overlap of the F-V relationships over their entire range when the 2/3 data is shifted by +14 pN along the force axis. In this way, the *inherent F-V* relationship of the motor in the absence of any internal forces can be obtained.

This inherent *F-V* curve shows that the packaging rate decreases even for small forces, indicating that the rate-limiting step in the motor's mechano-chemical cycle is force dependent and therefore involves a mechanical displacement. This behavior is different than that reported for RNA polymerase[10], but is similar to that found in the bacterial flagellar motor[11]. Within a Kramers model[12] of thermal activation over a single reaction barrier under the influence of force, our data imply that the rate-limiting step produces a conformational change of only ~0.1 nm (see supplemental data, Fig. V). This value is much smaller than the net movement of ~0.68 nm (2 bp) per ATP inferred from bulk studies[2]. Therefore, to the extent that this simple model applies, the rate-limiting step is force sensitive, but is not the main translocation step. Note that the velocity begins to decrease more sharply with force at ~45 pN, suggesting that a second step in the mechano-

chemical cycle of the motor, associated with a larger movement, becomes rate limiting at these higher forces.

Having separated the effects of the internal and external forces on the velocity of the motor, one can construct a histogram of the total force needed to stall it. As seen in Fig. 3c, the stall force ranges between 40 and 70 pN and has an average of ~57 pN, making ø29 one of the strongest molecular motors ever reported. This stall force is >8x higher than that reported for kinesin[13,14] and myosin motors[15], and >2x higher than that for RNA polymerase[10]. By multiplying the average stall force (57 pN) with the distance moved per ATP[2] (~0.68 nm), we obtain a work done per ATP of ~39 pN·nm. This yields an energy conversion efficiency of ~30% since the free energy associated with ATP hydrolysis is $\Delta G \cong 120$ pN·nm in our buffer[16]. This value falls within the range of efficiencies reported for myosin[15], kinesin[13,14], and RNA polymerase motors[10]. Additionally, the maximum observed force of 70 pN implies that the motor's step size must be less than ~5 bp (120 pN·nm / 70 pN≅1.7 nm).

Combining the rate dependence on external force (Fig. 3b) and on the fraction of DNA packaged (Fig. 1c), we can make a quantitative estimate of the build up of internal force as the prohead is filled. Fig. 3d shows that when the full genome has been packaged, this internal force reaches a surprisingly large value of about 50 pN. In many phages it is believed that the DNA is ordered as a spool in which the strands are packaged in a hexagonal lattice. By dividing the measured force by the hexagonal cell surface area, as determined by X-ray diffraction studies[17], one may obtain a rough estimate of a pressure of ~ 6 MPa inside the phage capsid, assuming that there is no significant energy dissipation in packaging. An osmotic pressure of similar order (~1 Mpa) has been reported to be necessary to condense DNA in solution to a density similar to that in the phage capsid[18]. If this 6 MPa pressure is transmitted to the capsid shell, the shell (thickness ~1.6 nm[1]) must have a tensile strength of at least ~100 MPa, a value similar to the bulk tensile strength for a typical aluminum alloy.

As seen in Fig. 3d, the force starts building only after about half of the ø29 genome is already packaged, a trend which has recently also been seen in simulations of DNA packaging into phage capsids[19]. Our finding suggests that the DNA does not immediately adopt its final condensed state inside the capsid, but instead is progressively compressed.

Also note that both the pause frequency and the internal pressure increase with DNA filling, indicating that the internal pressure may play a role in inducing pauses.

The compression of DNA in phage capsids has long been considered an intriguing phenomenon because it is thought to involve large energetic penalties[20,21]. An estimate of the total work done in packaging the ø29 genome is obtained by integrating the force curve in Fig. 3d, which yields 7.5 x 10^{-17} Joules (or 2 x 10^4 kT). This value can be compared with theoretical predictions for the equilibrium free energy change of the DNA. A model by Riemer and Bloomfield[20] gives 4 x 10^4 kT, while a preliminary estimate[22] based on a model by Odijk[21] yields ~5.6 x 10^3 kT. These predictions, which include electrostatic, bending and entropic penalties, but no dissipative effects, are of the same order of magnitude as our estimate of the total work done. Thus it is possible that a large fraction of the work done by the motor is reversible work and dissipation is not dominant. Moreover, the observations of rapid slipping of the DNA out of the capsid on a time scale of ~1/70 sec with no evidence of slower relaxation also suggest that there is little viscous resistance to DNA movement within the capsid.

While it has been argued that T7 phage relies on a motor for DNA injection into the host[23], other phages are known to passively eject their genome when exposed to the bacterial membrane receptor[17,24]. Our results lend support to a model for ø29 in which internal pressure provides the driving force DNA injection into the host cell for the first half of the injection process.

References:

1. Tao, Y. et al. Assembly of a tailed bacterial virus and its genome release studied in three dimensions. *Cell* **95**, 431-7 (1998).
2. Guo, P., Peterson, C. & Anderson, D. Prohead and DNA-gp3-dependent ATPase activity of the DNA packaging protein gp16 of bacteriophage phi 29. *J Mol Biol* **197**, 229-36 (1987).
3. Anderson, D. & Reilly, B. in *Bacillus subtilis and Other Gram-Positive Bacteria: Biochemistry, Physiology, and Molecular Genetics* (eds. Sonenshein, A., Hoch, J. A. & Losick, R.) 859-867 (American Society for Microbiology, Washington D.C., 1993).

4. Guo, P., Grimes, S. & Anderson, D. A defined system for in vitro packaging of DNA-gp3 of the Bacillus subtilis bacteriophage phi 29. *Proc Natl Acad Sci U S A* **83**, 3505-9 (1986).
5. Grimes, S. & Anderson, D. In vitro packaging of bacteriophage phi 29 DNA restriction fragments and the role of the terminal protein gp3. *J Mol Biol* **209**, 91-100 (1989).
6. Simpson, A. A. et al. Structure of the bacteriophage phi29 DNA packaging motor. *Nature* **408**, 745-50. (2000).
7. Ibarra, B. et al. Topology of the components of the DNA packaging machinery in the phage phi29 prohead. *J Mol Biol* **298**, 807-15. (2000).
8. Smith, S. B., Cui, Y. & Bustamante, C. Overstretching B-DNA: the elastic response of individual double- stranded and single-stranded DNA molecules. *Science* **271**, 795-9 (1996).
9. Barlow, R. *Statistics : a guide to the use of statistical methods in the physical sciences, p. 15-16* (Wiley, Chichester, England ; New York, 1989).
10. Wang, M. D. et al. Force and velocity measured for single molecules of RNA polymerase. *Science* **282**, 902-7 (1998).
11. Berg, H. C. & Turner, L. Torque generated by the flagellar motor of Escherichia coli. *Biophys J* **65**, 2201-16 (1993).
12. Kramers, H. Brownian motion in a field of force and the diffusion model of chemical reactions. *Physica* **7**, 284 (1940).
13. Svoboda, K. & Block, S. M. Force and velocity measured for single kinesin molecules. *Cell* **77**, 773-84 (1994).
14. Coppin, C. M., Pierce, D. W., Hsu, L. & Vale, R. D. The load dependence of kinesin's mechanical cycle. *Proc Natl Acad Sci U S A* **94**, 8539-44 (1997).
15. Finer, J. T., Simmons, R. M. & Spudich, J. A. Single myosin molecule mechanics: piconewton forces and nanometre steps. *Nature* **368**, 113-9 (1994).
16. Lehninger, A. L., Nelson, D. L. & Cox, M. M. *Principles of biochemistry, p. 375* (Worth Publishers, New York, NY, 1993).
17. Earnshaw, W. C. & Casjens, S. R. DNA packaging by the double-stranded DNA bacteriophages. *Cell* **21**, 319-31. (1980).

18. Rau, D. C., Lee, B. & Parsegian, V. A. Measurement of the repulsive force between polyelectrolyte molecules in ionic solution: hydration forces between parallel DNA double helices. *Proc Natl Acad Sci U S A* **81**, 2621-5. (1984).
19. Kindt, J., Tzlil, S., Ben-Shaul, A., & Gelbart, W. M. personal communication.
20. Riemer, S. C. & Bloomfield, V. A. Packaging of DNA in Bacteriophage Heads: Some Considerations on Energetics. *Biopolymers* **17**, 785-794 (1978).
21. Odijk, T. Hexagonally packed DNA within bacteriophage T7 stabilized by curvature stress. *Biophys J* **75**, 1223-7 (1998).
22. Odijk, T. personal communication.
23. Garcia, L. R. & Molineux, I. J. Transcription-independent DNA translocation of bacteriophage T7 DNA into Escherichia coli. *J Bacteriol* **178**, 6921-9. (1996).
24. Novick, S. L. & Baldeschwieler, J. D. Fluorescence measurement of the kinetics of DNA injection by bacteriophage lambda into liposomes. *Biochemistry* **27**, 7919-24. (1988).
25. Grimes, S. & Anderson, D. The bacteriophage phi29 packaging proteins supercoil the DNA ends. *J Mol Biol* **266**, 901-14 (1997).
26. Bjornsti, M. A., Reilly, B. E. & Anderson, D. L. Morphogenesis of bacteriophage phi 29 of Bacillus subtilis: oriented and quantized in vitro packaging of DNA protein gp3. *J Virol* **45**, 383-96 (1983).
27. Baumann, C. G., Smith, S. B., Bloomfield, V. A. & Bustamante, C. Ionic effects on the elasticity of single DNA molecules. *Proc Natl Acad Sci U S A* **94**, 6185-90 (1997).

Acknowledgements. We thank W. M. Gelbart, P. Jardine, T. Odijk, V. Bloomfield, D. Frenkel, C. Varga, and Mark Young for insightful comments. This research was supported in part by NIH grants GM-32543, DE-03606 and GM-59604, DOE grant DE-FG03-86ER60406, and NSF grants MBC-9118482 and DBI-9732140. D.E.S. and S.J.T. are supported by a grant from the Packard Foundation. S.J.T. is supported by the Netherlands Organization for Scientific Research (NWO).

Correspondence should be addressed to C.B. (carlos@alice.berkeley.edu).

Figure Captions

Fig. 1a, Three schematic diagrams indicating: The experimental set-up at the start of a measurement, "constant force feedback" mode, and "no feedback" mode measurements. A single ø29 packaging complex is tethered between two microspheres. Optical tweezers were used to trap one microsphere and measure the forces acting on it, while the other microsphere was held by a micropipette. To insure measurement on only one complex, the density of complexes on the microsphere is adjusted so that only about one out of 5-10 microspheres yielded hookups. Hookups broke in one discrete step as the force was increased, indicating only one DNA molecule carried the load. **b,** Plots of DNA tether length vs. time for four different complexes with a constant force of ~5pN using a 34.4 kb ø29-λ DNA construct. **Inset,** Blowups of blue and black lines of regions indicated by arrows, showing pauses (curves have been shifted). The solid lines are a 100 point average of the raw data. For statistical analysis, a pause is scored if the rate is <10 bp/s. for more than 0.5 s. This threshold allowed us to reliably score the observed plateaus in the length vs. time plots that occur during pauses. Features occurring on a shorter time scale and having a slope >10 bp/s could not be reliably discerned as pauses. Analysis shows the mean duration of pauses is 4.0 s (σ=5.1 s, n=425). Histograms of the distributions of pause duration and time intervals between pauses are given in the supplemental data section, Fig. II. **c,** Packaging rate vs. the amount of DNA packaged, relative to the original 19.3 kb ø29 genome. Grey line, trace for a single complex (derived from black trace in panel b). Rates were obtained by linear fitting in a 1.5 sec sliding window. The thick red line is an average of 8 such measurements. Here, large pauses (velocity drops >30 bp/s below local average) were removed, and the curves were horizontally shifted to account for differences in microsphere attachment points. The red line was smoothed using a 200 nm sliding window. The standard deviation for the ensemble of measurements varies from ~20 bp/s at the beginning down to ~10 bp/s at the end.

Fig. 2 Measurements of packaging in "no feedback" mode: **a**, The tether shortens (blue line), and the force increases (red line) as the portal motor pulls in the DNA. In this example the motor stalled at a force of ~55 pN. While in many measurements the linkage

broke before stalling was observed, similar stall forces could be projected from these curves. We suspect that such breakage events occur at the antibody-prohead connection. **inset,** Spontaneous slipping events, where the DNA comes out of the capsid, were accompanied with abrupt decreases in force.

Fig. 3, Force-Velocity (*F-V*) analysis: **a,** The packaging rate for a single complex (thin gray line) was determined by linear fitting of the data in Fig. 2 in a 0.7 s sliding window. The thick black line is obtained by editing out large pauses (marked by '*'; velocity drops >30 bp/s below local average; <2% of the data) and smoothing (50 point sliding window). These long pauses were removed so as not to perturb the general trend of the FV behavior. The red and blue lines are data from two other complexes. **b,** Mean *F-V* curves when ~1/3 of the genome is packaged (red line) and when ~2/3 of the genome is packaged (leftmost blue line). These curves were obtained from 14 and 8 individual traces, respectively. Arrows show the blue line being shifted by +14 pN to account for the internal force (see text). **c,** Histogram of total stall force measured for 65 individual complexes indicates an average stall force of ~57 pN. DNA over-stretching was not observed because linkages always broke at external forces lower than 65 pN. However, stall forces above 65 pN could be determined in cases where internal force added to the total force. **d,** The internal force versus the percentage of the genome packaged. This plot is obtained by relating the packaging rate in Fig. 1c to the force acting on the motor using the *F-V* relationship in Fig. 3b, while accounting for the 5 pN of external load in the data of Fig. 1c.

Methods

Stalled Packaging Complexes. Components of the ø29 in-vitro packaging assay, including proheads, DNA-gp3, and gp16 were purified as described previously[25]. The 19.3 kb ø29 DNA-gp3 (6.6 μm in length) is cut with *Nco*I-A to yield a 15 kb left end ("ø29-*Nco*I-A DNA") and a 4.3 kb right end. The left end is preferentially packaged[5,26]. These fragments are biotinylated using the Klenow fragment of DNA Polymerase I (exo- mutant, New England Biolabs) to incorporate biotin-14-dATP and biotin-14-dCTP (Gibco). The longer 34.4 kb ø29–λ DNA is constructed by ligating together the ø29 and λ *Nco*I-A fragments. Prior to ligation, the cos site of λ DNA is biotinylated as described above. To

initiate a packaging reaction we add 4 µl of 0.25 mM ATP (Roche) to a 13.5 µl solution of buffer A (50 mM Tris-HCl buffer (pH 7.8), 50 mM NaCl, 5 mM $MgCl_2$), 0.1 µg of biotinylated DNA-gp3, 0.5 µg gp16, and 10 µg ø29 proheads. This mixture is incubated for ~30 seconds, and then the packaging is stalled by adding 4 µl of 2.5 mM γS-ATP (Roche), such that the genome is partly prepackaged. These complexes are stable for >10 hours and are reactivated during the measurement by exposing them to buffer A plus 0.5 mM ATP, 5 µM ADP, 5 µM NaH_2PO_4 (source of phosphate ions) and 50 µg/ml BSA. This ATP concentration is saturating (increasing it by a factor of ten does not significantly increase the packaging rate, i.e. the reaction is not diffusion limited).

Microsphere Preparation. Streptavidin coated polystyrene microspheres (2.2 µm diam, 0.5% w/v, Spherotech) are washed twice and pre-blocked for 5 minutes with 5 mg/ml BSA in Buffer A. Stalled complexes are attached to the microspheres (via the biotinylated DNA) by adding approximately 0.3 µl of the stalled reaction mixture and 1 µl of RNase inhibitor (SuperaseIn, Ambion) to 20 µl of microspheres and incubating for 15-20 minutes. The microspheres are then diluted in 1 ml buffer A. Protein G coated polystyrene microspheres (2.8 µm diam, 5% w/v, Spherotech) are washed twice in phosphate buffered saline and incubated for >20 min with a ~1/10 dilution of rabbit antisera prepared against ø29. 5 µl of microspheres (washed five times) and 1 µl of RNase inhibitor are added to 1 ml of buffer A.

Optical Tweezers. We use a dual-beam optical tweezers apparatus similar to that described previously[8]. The measured trap stiffness is ~0.12 pN/nm and the force is recorded at a rate of ~70 Hz. The displacements of the trapped microsphere were derived from the measured forces. The pulling angle could be varied over a 120° range but did not appear to affect the packaging rate. The pipette position is recorded using an optical lever having a resolution of ~1 nm. The contour length of the DNA (in base pairs) is determined from the measured force and end-to-end distance and using the worm-like-chain model assuming a persistence length of 53 nm, a stretch modulus of 1200 pN and a distance per base pair of 0.34 nm[27].

Figure 1a

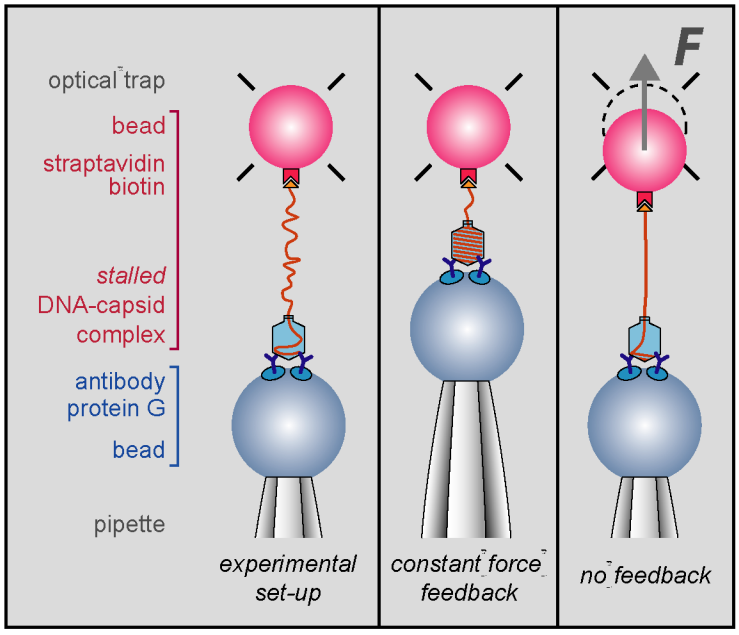
optical trap
bead
straptavidin
biotin
stalled
DNA-capsid
complex
antibody
protein G
bead
pipette
F
experimental set-up
constant force feedback
no feedback

Figure 1

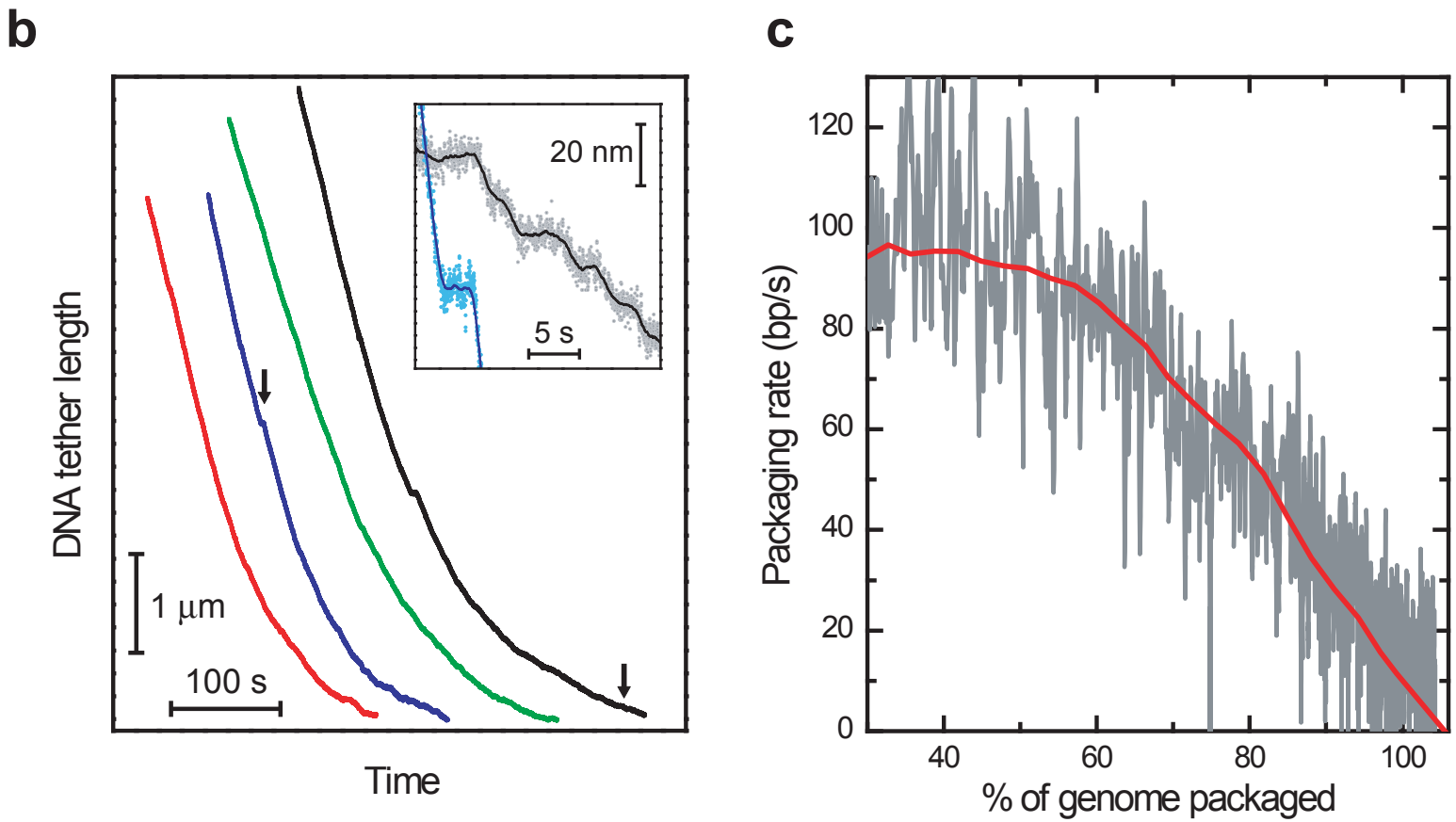
b
DNA tether length
Time
1 μm
100 s
20 nm
5 s
c
Packaging rate (bp/s)
% of genome packaged
0
20
40
60
80
100
120
40
60
80
100

Figure 2

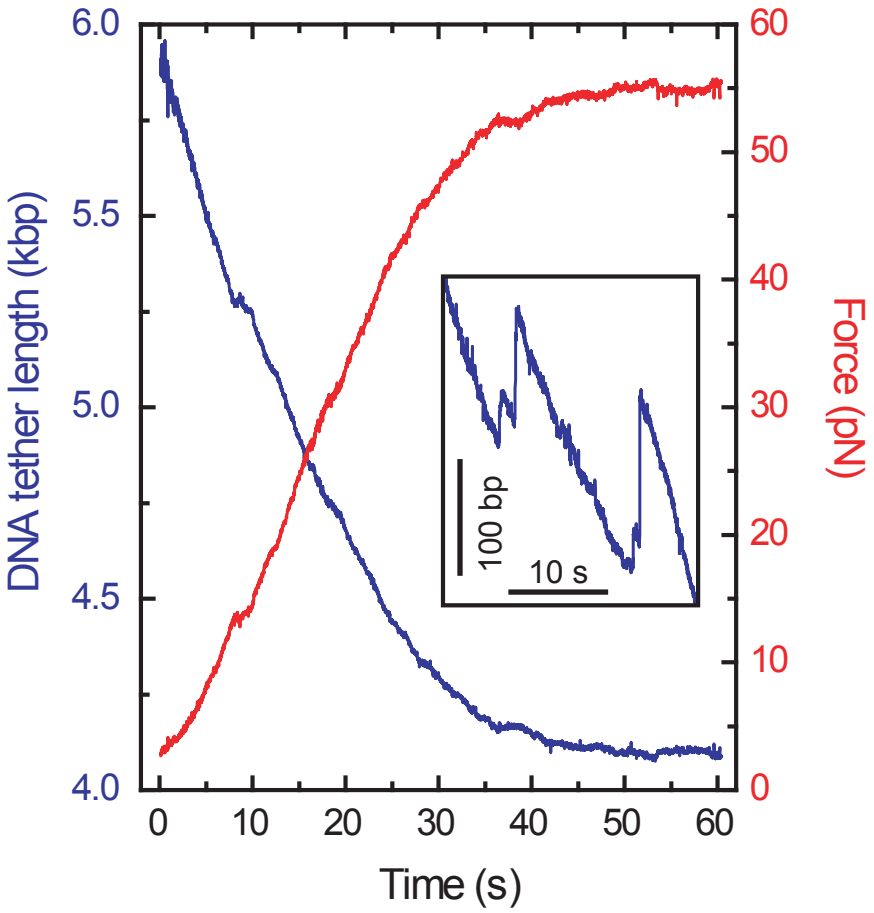
6.0
5.5
5.0
4.5
4.0
DNA tether length (kbp)
60
50
40
30
20
10
0
Force (pN)
0
10
20
30
40
50
60
Time (s)
100 bp
10 s

Figure 3

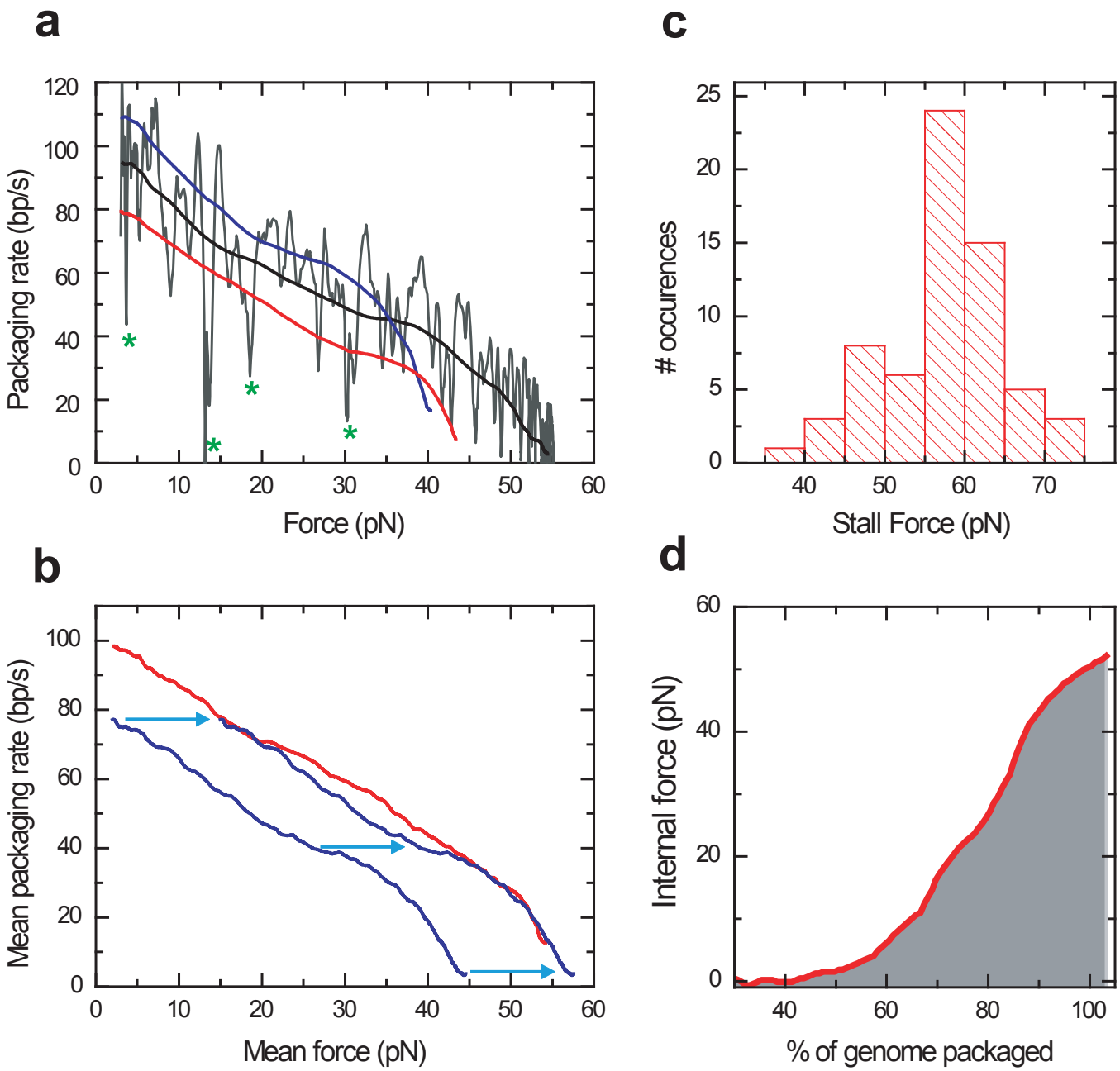
a
Packaging rate (bp/s)
Force (pN)
b
Mean packaging rate (bp/s)
Mean force (pN)
c
occurences
Stall Force (pN)
d
Internal force (pN)
% of genome packaged